Radicals Generated in Tetramolecular Guanine Quadruplexes by Photoionization: Spectral and Dynamical Features

Akos Banyasz, Evangelos Balanikas, Lara Martinez-Fernandez, Gérard Baldacchino, Thierry Douki, Roberto Improta, Dimitra Markovitsi

THE JOURNAL OF PHYSICAL CHEMISTRY B

Article

Cite This: J. Phys. Chem. B 2019, 123, 4950−4957

pubs.acs.org/JPCB

Radicals Generated in Tetramolecular Guanine Quadruplexes by Photoionization: Spectral and Dynamical Features

Akos Banyasz,[†,‡] Evangelos Balanikas,[†] Lara Martinez-Fernandez,[†,§] Gérard Baldacchino,[†] Thierry Douki,[∥] Roberto Improta,[†,⊥] and Dimitra Markovitsi*[,†]

[†]LIDYL, CEA, CNRS, Université Paris-Saclay, F-91191 Gif-sur-Yvette, France

[‡]Univ Lyon, ENS de Lyon, CNRS UMR 5182, Université Claude Bernard Lyon 1, Laboratoire de Chimie, F-69342 Lyon, France

[§]Departamento de Química, Universidad Autónoma de Madrid, c/ Francisco Tomás y Valiente 7, Cantoblanco, 28049 Madrid, Spain

[∥]Univ. Grenoble-Alpes, CEA, CNRS, SyMMES UMR, 5819 Grenoble, France

[⊥]Istituto Biostrutture e Bioimmagini−Consiglio Nazionale delle Ricerche, Via Mezzocannone 16, I-80134 Napoli, Italy

Supporting Information

ABSTRACT: G-quadruplexes are four-stranded DNA structures playing a key role in many biological functions and are promising for applications in the field of nanoelectronics. Characterizing the generation and fate of radical cations (electron holes) within these systems is important in relation to the DNA oxidative damage and/or conductivity issues. This study focuses on guanine radicals in G-quadruplexes formed by association of four TGGGGT strands in the presence of Na^+ cations, $(TG4T)_4/Na^+$. Using nanosecond transient spectroscopy with 266 nm excitation, we quantitatively characterize hydrated ejected electrons and three types of guanine radicals. We show that, at an energy lower by 2.7 eV than the guanine ionization potential, one-photon ionization occurs with quantum yield of $(3.5 \pm 0.5) \times 10^{-3}$. Deprotonation of the radical cations is completed within 20 μs, leading to the formation of $(G\text{-}H2)^\bullet$ radicals, following a strongly nonexponential decay pattern. Within 10 ms, the latter undergoes tautomerization to deprotonated $(G\text{-}H1)^\bullet$ radicals. The dynamics of the various radicals determined for $(TG4T)_4/Na^+$, in connection to those reported previously for telomeric G-quadruplexes TEL21/Na^+, is correlated with energetic factors computed by quantum chemical methods. The faster deprotonation of radical cations in $(TG4T)_4/Na^+$ compared to TEL21/Na^+ explains that irradiation of the former does not generate 8-oxodGuo, which is readily detected by high-performance liquid chromatography/mass spectrometry in the case of TEL21/Na^+.

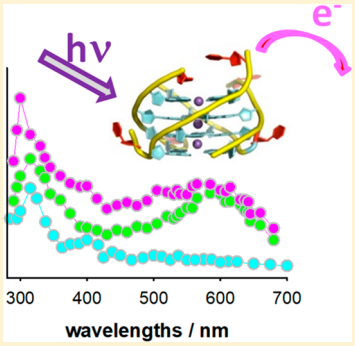

INTRODUCTION

G-quadruplexes are noncanonical structures of nucleic acids formed by guanine-rich DNA/RNA strands.[1] Their building blocks are tetrads composed of four guanines interconnected through eight hydrogen bonds (Figure 1a), while metal ions located in the central cavity contribute to their stability. Detected recently in vivo,[2,3] they play a key role in various biological functions, such as gene transcription and cell division, and are targets for cancer therapy.[4] In parallel, G-quadruplexes have attracted attention for their potential applications in the field of molecular electronics.[5,6] In both biological and technological fields, oxidation of guanine, which has the lowest oxidation potential among nucleobases, is a key issue. On the one hand, oxidatively generated damage may alter the functioning of G-quadruplexes within cells.[7,8] On the other hand, nanodevices search to exploit charge transport involving electron holes.[9,10] In all these cases, guanine radical cations, generated in various ways (through chemical reactions with electron donors, through electric junctions, electrochemically...) are main players. However, guanine radical cations in neutral pH are also known to be metastable, undergoing rapid

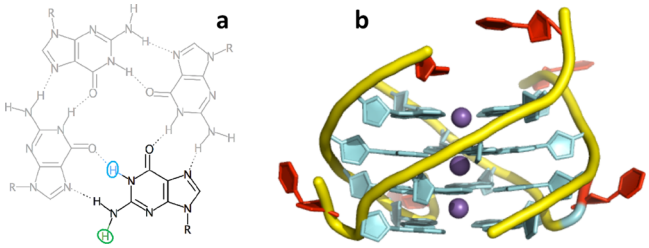

Figure 1. Schematic representation of the guanine tetrad (a) and the studied $(TG4T)_4/Na^+$ G-quadruplex (b). Loss of the blue or the green proton shown in (a) leads to formation of $(G\text{-}H1)^\bullet$ or $(G\text{-}H2)^\bullet$ radical, respectively. (b) Cyan: 2′-deoxyguanosines; red: thymidines; yellow: phosphoribose backbone; violet: Na^+ ions in the central cavity.

Received: March 20, 2019
Revised: May 7, 2019
Published: May 22, 2019

DOI: 10.1021/acs.jpcb.9b02637
J. Phys. Chem. B 2019, 123, 4950−4957

deprotonation.[11−13] Such deprotonation disrupts charge transport in guanine wires and may also modify the radical reactivity, thus affecting the types of lesions that are ultimately created in DNA.[14,15]

Within the above described context, it is very important to determine the lifetime of guanine radicals within G-quadruplexes. So far, very few studies, performed by nanosecond transient absorption, have tackled these questions. Su and co-workers examined guanine radicals generated in several four-stranded structures by one-electron oxidation reaction with sulfate anion.[16] They drew two important conclusions: (i) radical deprotonation in G-quadruplexes is by 1−2 orders of magnitude slower compared to what happens in the case of the mononucleotide 2′-deoxyguanosine 5′-monophosphate (dGMP); (ii) in contrast to dGMP, for which deprotonation of the radical cation $(G)^{+\bullet}$ occurs at position 1 leading to $(G\text{-}H1)^{\bullet}$ radical,[11−13] deprotonation in G-quadruplexes gives rise to $(G\text{-}H2)^{\bullet}$ radicals (Figure 1a). Both conclusions were qualitatively confirmed by our study on G-quadruplexes formed by folding of the human telomeric sequence $GGG(TTAGGG)_3$ in the presence of Na^+ ions ($TEL21/Na^+$).[17] In our approach, radicals are produced by photoionization of G-quadruplexes, avoiding bimolecular reactions with external molecules. By quantifying the ejected electrons and the parent radicals, we were able to follow the survival probability of the latter over five decades of time and evidence complex transformations, including $(G\text{-}H2)^{\bullet} \rightarrow (G\text{-}H1)^{\bullet}$ tautomerization.

A last but not least outcome of our study on $TEL21/Na^+$ was that photons with significantly lower energy than the ionization potential of DNA bases[18] are capable of generating guanine radicals when they are directly absorbed by human telomere G-quadruplexes.[17] The quantum yield of one-photon ionization at 266 nm was found to be 4.5×10^{-3}. This value is 3−4 times higher than those determined for DNA duplexes under the same experimental conditions,[19−21] suggesting that telomeres are particularly vulnerable toward UV-induced oxidative damage.

As G-quadruplexes are known to adopt different types of topology,[22] it is fundamental to understand how structural factors affect both radical generation upon direct absorption of low-energy photons and characterize their lifetime. The present work focuses on G-quadruplexes formed by association of four TGGGGT strands in the presence of Na^+ ions, abbreviated as $(TG4T)_4/Na^+$ (Figure 1b). Within these four-stranded scaffolds, guanines adopt a parallel arrangement with respect to the glycosidic bond while an antiparallel arrangement is encountered in $TEL21/Na^+$.[23] The main tool of our study is transient absorption spectroscopy using 266 nm excitation with low excitation intensities ($\leq$2 MW cm^{-2}). Three aspects of our methodology are essential: (i) the probed electrons stem solely from DNA and not from the aqueous solvent; (ii) the ejected electrons are scavenged by the phosphate groups of the buffer, preventing nucleophilic attack to DNA;[24,25] (iii) the radical concentration is at least 15 times lower than that of the G-quadruplex, precluding biradical interactions.

The experimental spectra are assigned with the help of theoretical spectra computed by the time-dependent differential functional theory (TD-DFT). In our calculations, we consider the whole G-quadruplex structure through quantum mechanics/molecular mechanics (QM/MM) approach. In this way, we examine at what extent interaction within DNA multimers may modify key spectral features of various types of radicals.[17,19,20,26]

METHODS

Experimental Section. TGGGGT oligonucleotides, purified by reversed-phase high-performance liquid chromatography and tested by matrix-assisted laser desorption/ionization−time-of-flight analysis, were purchased from Eurogentec Europe. G-quadruplexes were prepared in a dry bath (Eppendorf-ThermoStatplus). To this end, the lyophilized oligomer was dissolved in 2 mL of phosphate buffer (0.15 mol L^{-1} NaH_2PO_4, 0.15 mol L^{-1} Na_2HPO_4, pH 7) that is prepared using ultrapure water delivered by a millipore (Milli-Q Integral) system; the solution was heated to 96 °C during 5 min, cooled to the melting point (cooling time: 1 h), where the temperature was maintained for a 10 min; subsequently, the solution was cooled to 4 °C (cooling time: 2 h), where it was incubated for 1 week. G-quadruplex formation was checked by recording the melting curve at 295 nm,[27] shown in Figure S1.

The pH was measured by a Hanna Instr. Apparatus (pH 210). It was adjusted to 7 by addition of a concentrated NaOH solution. For measurements of the G-quadruplex in pH 3, about 30 μL of the mother solution (pH 7) were added into 2 mL of NaCl solution with the same ionic strength; subsequently, the pH was adjusted by addition of a concentrated HCl solution. Steady-state absorption spectra were recorded using a Lambda 850 (PerkinElmer) spectrophotometer.

Time-resolved experiments were performed using a homemade nanosecond flash photolysis setup; the excitation source was the fourth harmonic of a Nd/YAG laser (Spectra-Physics, Quanta Ray). The excited area at the surface of the sample and optical path length on the excitation side were, respectively, 0.6 × 1.0 cm^2 and 0.1 cm. The analyzing beam (150 W Xe-arc lamp, OSRAM XBO) passed through the sample at right angle with respect to the exciting beam, dispersed in a Jobin-Yvon SPEX 270M monochromator, detected by a Hamamatsu R928 photomultiplier and recorded by Lecroy Waverunner oscilloscope (6050A or 6084). Experiments on the sub μs-scale were performed by intensifying the Xe-arc lamp via an electric discharge. Transient absorption spectra were recorded using a wavelength-by-wavelength approach. Typically, at each wavelength, a series of three successive signals, resulting from 50 to 150 laser shots each, were recorded; if judged to be reproducible, they were averaged to reduce the signal-to-noise ratio. Fast shutters were placed in the path of both laser and lamp beams; thus, the excitation repetition rate was decreased from 10 to 0.2 Hz. The absorbance on the excitation side was 0.25 ± 0.02 over 0.1 cm, corresponding to a G-quadruplex concentration of about 1.5×10^{-5} mol L^{-1}. At the maximum excitation intensity (2 MW cm^{-2}), the concentration of ejected electrons was $\sim 10^{-6}$ mol L^{-1}. During the experiments, the temperature was kept at 23 ± 0.5 °C. The incident pulse energy at the surface of the sample was measured using a NIST traceable pyroelectric sensor (OPHIR Nova2/PE25); it was cross-checked by measuring the absorbance of the naphthalene triplet state, whose quantum yield in cyclohexane is 0.75.[28] Ar-purged samples were used for photoionization experiments. As we found that the decays on the μs to ms domains were not affected by oxygen, transient absorption spectra were determined in aerated conditions.

Theoretical Section. The minima of the ground-state geometry were optimized using mixed QM/MM calculations;

DOI: 10.1021/acs.jpcb.9b02637
J. Phys. Chem. B 2019, 123, 4950−4957

three of the four guanine tetrads and the inner Na^+ ions were described at the QM level, whereas the fourth tetrad, the backbone and outer Na^+ atoms were described at the MM level (Figure S2). The method selected for the QM region was DFT, adopting the M052X functional[29,30] combined with the 6-31G(d) basis set, which has been already profitably used to describe DNA duplex and quadruplexes.[17,31,32] The MM part was described via Amber parm96.dat force field.[33] This is done using the ONIOM procedure, as implemented in Gaussian09.[34] Solvation was taken into account for the whole QM/MM system using the polarizable continuum model (PCM).[35,36]

Using the experimental X-ray structure as a starting point,[37] we optimized the cation and (PT3loc)[26] and, then, starting from this minimum, the ground-state geometry of the deprotonated $(G\text{-}H1)^\bullet$ and $(G\text{-}H2)^\bullet$ species.

Absorption spectra at the optimized minima were computed by resorting to the time-dependent version of DFT (TD-DFT) with the same approach used in the ground-state calculations, TD-M052X/6-31G(d) and MM (Amber/parm96.dat), for the QM and MM parts, respectively. For easier comparison with the experimental results, the computed absorption spectra were simulated by convoluting each electronic transition with a Gaussian function (half width at half maximum: 0.3 eV) and shifted by −0.6 eV. The −0.6 value corresponds to the shift required so that the spectrum of 2′-deoxyguanosine in water, computed at the same level of theory adopted herein, coincides with the experimental spectrum. Nevertheless, not all of the sources of error (functional, incomplete basis set and lack of vibronic and thermal effects) would need the same shift. We note that smaller energy shifts (0.2−0.3 eV) were found in a recent study of radicals in the guanine−cytosine base-pair;[38] the latter work used larger basis sets, that are not affordable for calculations on G-quadruplexes, which are much bigger systems.

RESULTS AND DISCUSSION

Hydrated Electrons. Electrons issued from photoionization in aqueous solution are known to be hydrated in less than 1 ps.[40] Hydrated electrons exhibit a broad absorption band peaking around 720 nm with a maximum molar absorption coefficient ε_{max} of 19 700 mol^{-1} L cm^{-1}.[39] Based on this property, we quantify the hydrated ejected electrons by probing their transient absorption on the sub-microsecond timescale (Figure 2a). Under the same experimental conditions, no signal was detected from the neat solvent, showing that electrons stem only from the G-quadruplex. The hydrated electron decays are fitted with monoexponential functions $A_0 + A_1 \exp(-t/\tau_1)$. The τ_1 values found for $(TG4T)_4/Na^+$ in pH 7 and pH 3 are, respectively, 0.5 ± 0.1 and 0.15 ± 0.05 μs. Such short time constants result from reaction of hydrated electrons with phosphate groups and hydronium ions.[41] The A_1 value, divided by the ε_{max} (19700 mol^{-1} L cm^{-1})[39] provides the initial concentration of hydrated electron $[e^-]_0$.

Although the excitation intensity is much lower compared to that used in previous studies on DNA photo-ionization,[42−44] two-photon effects are not avoided. To disentangle between one- and two-photon processes, we vary the excitation intensity, resulting in different concentrations of absorbed photons $[h\nu]$. Subsequently, we plot $[e^-]_0/[h\nu]$ versus $[h\nu]$, obtaining the so-called ionization curve (Figure 2b). The fit with a linear function $[e^-]_0/[h\nu] = \varphi_1 + \alpha[h\nu]$ provides the quantum yield for one photon ionization φ_1, while the two photon ionization yield is given by the slope of the curve, $\varphi_2 = \alpha[h\nu]$. We note that, within the precision of our measurements, the signal intensities at 700 and 720 nm were practically identical. Therefore, the ionization curves were derived from the 700 nm decays, which are less noisy compared to those at 720 nm.

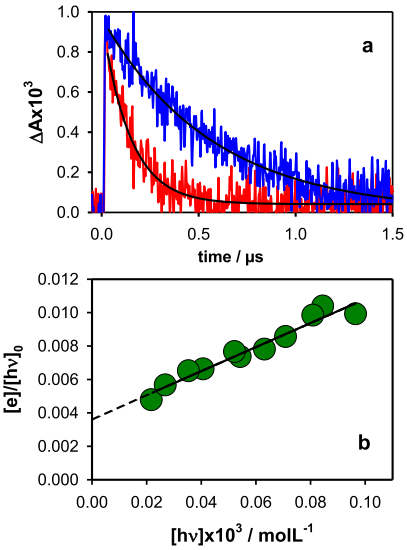

Figure 2. Quantification of ejected electrons in Ar-saturated conditions. (a) Normalized transient absorption signals recorded at 700 nm for $(TG4T)_4/Na^+$ in pH 3 (red) and pH 7 (blue); black lines correspond to fits with model functions $A_0 + A_1 \exp(-t/\tau_1)$ with τ_1 values of 0.15 and 0.5 μs, respectively. (b) Ionization curve obtained for $(TG4T)_4/Na^+$ in pH 7; $[e^-]_0$ and $[h\nu]$ denote, respectively, the zero-time concentration of hydrated ejected electrons and the concentration of absorbed photons per laser pulse; $[e^-]_0$ is determined using the A_1 values and a molar absorption coefficient of 19 700 mol^{-1} L cm^{-1}.[39] Experimental points (circles) are fitted with the linear function $[e^-]_0/[h\nu] = \phi_1 + \alpha[h\nu]$ (black).

For $(TG4T)_4/Na^+$ in pH 3, we determined solely $[e^-]_0$ for a given excitation intensity to correlate it with that of radical cations (see below). The ionization curve shown in Figure 2b was obtained for $(TG4T)_4/Na^+$ in pH 7, which gives a $\varphi_1 = (3.5 \pm 0.5) \times 10^{-3}$. This value is clearly higher than those reported previously for a few model single and double helices, which fall in the range $(1-2) \times 10^{-3}$,[19−21,45] but lower than that determined for $TEL21/Na^+$, $\varphi_1 = (4.5 \pm 0.6) \times 10^{-3}$.[17]

Radicals. As we saw previously, experiments on the sub-microsecond timescale provide quantification of the hydrated ejected electrons. After their decay, the time-resolved absorption spectra observed for $(TG4T)_4/Na^+$ are expected to correspond to radicals issued from photoionization and, possibly, to photoreaction products.

The spectral identification of the various types of radicals, for example, the radical cation $(G)^{+\bullet}$ and deprotonated radicals $(G\text{-}H1)^\bullet$ and $(G\text{-}H2)^\bullet$, including their quantification via their molar absorption coefficients, associated with $[e^-]_0$, allows us to determine their survival probability. Before presenting the radical spectra obtained for the G-quadruplex in neutral buffered solution, we discuss the spectrum of the radical cation determined experimentally by photoionization of the system in pH 3; under these conditions, deprotonation of $(G)^{+\bullet}$ is hindered,[11] whereas the ground-state absorption spectrum remains the same as in pH 7 (Figure S3).

DOI: 10.1021/acs.jpcb.9b02637
J. Phys. Chem. B 2019, 123, 4950−4957

Spectral Features. *Experiments at pH 3.* We recorded the spectrum of the $(TG4T)_4/Na^+$ radical cation at 2.5 μs (Figure 3), to compare it with that obtained for the G-quadruplex in

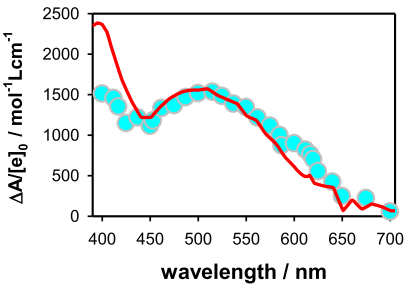

Figure 3. Transient absorption spectrum recorded for $(TG4T)_4/Na^+$ in pH 3 at 2.5 μs (circles); the measured differential absorbance has been divided by the concentration of ejected electrons, determined in the same experiment. Average of three independent experiments. The red line corresponds to the spectrum of the radical cation of dGMP, represented with its molar absorption coefficient.[46]

neutral pH. We also evaluated its molar absorption coefficient assuming that the radical cation concentration matches that of the hydrated electrons $[e^-]_0$, determined as explained in the previous section. The molar absorption coefficient of the $(TG4T)_4/Na^+$ radical cation (Figure 3) coincides with that of the monomeric analog at 500 nm, but at 400 nm it is ca. 40% lower. A lower intensity of the latter band with respect to the dGMP cation was also found in the case of $TEL21/Na^+$ (Figure 10 in ref 17). Moreover, the $(TG4T)_4/Na^+$ radical cation spectrum is more intense around 600 nm than those of both dGMP (Figure 3) and $TEL21/Na^+$ radical cations (Figure S4). Note that the experimental spectrum of the $(TG4T)_4/Na^+$ radical cation (Figure 4) is blue-shifted

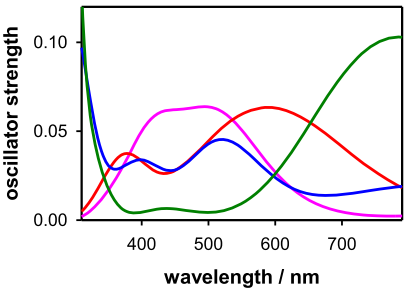

Figure 4. Comparison of the spectra computed for $(TG4T)_4/Na^+$ radicals. Pink: radical cation localized on a single guanine;[26] red: radical cation delocalized over two guanines,[26] green: $(G\text{-}H2)^\bullet$ deprotonated radical; blue $(G\text{-}H1)^\bullet$ deprotonated radical.

compared to that published recently for the same system.[26] The reason is that, because of a technical failure of the pH-meter, discovered later, the effective pH value in the previous study was close to 6.

The small but clearly distinguishable feature around 600 nm in Figure 3 is correlated with delocalization of the electron hole over two guanines occurring for a small part of the population.[26] Quantum chemical calculations predict that such charge delocalization is possible only for G-quadruplex structures with parallel arrangement but not for antiparallel structures.[26,47] The spectra computed for $(TG4T)_4/Na^+$ bearing localized and delocalized electron holes,[26] shown in Figure 4, present clear differences, with the latter exhibiting an important band at longer wavelengths.

Experiments at pH 7. The time-resolved absorption spectra of $(TG4T)_4/Na^+$ in pH 7 exhibit important evolution during the time. Typical examples are presented in Figure 5; similar

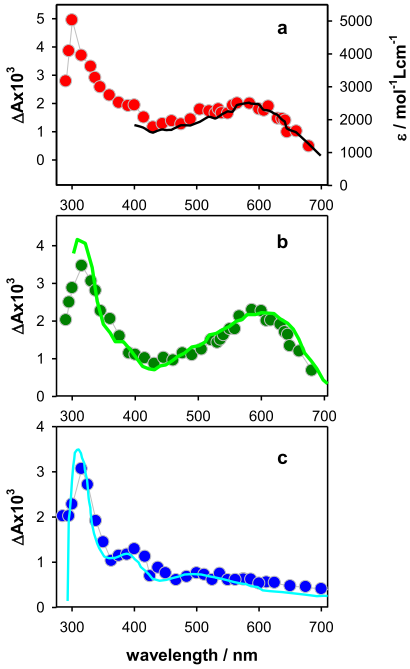

Figure 5. Transient absorption spectra recorded for $(TG4T)_4/Na^+$ in pH 7 (circles) at 2.5 μs (a), 50 μs, (b) and 6 ms (c). Excitation intensity: 2 MW cm^{-2}. The black line in (a) is a linear combination of the $(TG4T)_4/Na^+$ spectra corresponding to its radical cation (Figure 3) and the $(G\text{-}H2)^\bullet$ deprotonated radical (Figure 5b) at a ratio 25:75. The green (b) and cyan (c) lines correspond, respectively, to the spectra of $(G\text{-}H2)^\bullet$[48] and $(G\text{-}H1)^\bullet$[46] radicals of monomeric guanosine, their intensity being arbitrarily normalized with respect to that of the G-quadruplex spectra.

spectra, but with increasing experimental error, are obtained at lower excitation intensities when the ratio ϕ_2/ϕ_1 decreases from 1.7 to 1.2. At the earliest probed time (2.5 μs), the spectrum exhibits a broad band in the visible spectral domain and more intense one around 300 nm. As time passes by, the relative intensity of the UV band with respect to that in the visible spectral domain decreases significantly, dropping from 2.5 to 1.5 at 50 μs. In parallel, the band in the visible spectral domain becomes narrower and shifts slightly toward the red. The spectrum at 50 μs strongly resembles that reported in the literature for $(G\text{-}H2)^\bullet$ radicals of monomeric guanosine derivatives.[46,48] Thus, we assign it to the $(G\text{-}H2)^\bullet$ radical. Further transformations take place in the ms time-scale. At 6 ms, the spectral profile has completely changed. We now distinguish three bands of decreasing intensity, peaking at 315, 400, and 515 nm, as reported for the $(G\text{-}H1)^\bullet$ radical of dGMP.[46,49]

From the above observations, we can already draw a rough picture of the successive events taking place on the probed timescale. First, we have a mixture of the radical cation and deprotonated radical $(G\text{-}H2)^\bullet$. After completion of the deprotonation process, only $(G\text{-}H2)^\bullet$ radicals are present. Finally, at least part of the latter radicals undergoes tautomerization, giving rise to $(G\text{-}H1)^\bullet$ radicals. These

DOI: 10.1021/acs.jpcb.9b02637
J. Phys. Chem. B 2019, 123, 4950−4957

assignments are supported by the comparative spectra computed for the various $(TG4T)_4/Na^+$ radicals, as shown in Figure 4. The most intense band in the red is indeed exhibited by $(G\text{-}H2)^\bullet$, located close to that of the delocalized radical cation. The spectrum of $(G\text{-}H1)^\bullet$ is characterized by two bands which are blue-shifted with respect that of $(G\text{-}H2)^\bullet$; weaker transitions, located at lower energies could be responsible for the important red tail observed experimentally (Figure 5c), as in the case of the guanine deprotonated radical cations in alternating GC duplexes.[19]

As mentioned previously, the important width of the absorption band observed at 2.5 μs for $(TG4T)_4/Na^+$ in pH 7 suggests the coexistence of the radical cation and $(G\text{-}H2)^\bullet$ deprotonated radical. To quantify the relative concentrations of these species, we constructed linear combinations of the spectra corresponding to the radical cation (Figure 3, 2.5 μs) and the deprotonated radical $(G\text{-}H2)^\bullet$ (Figure 5b); for the latter spectrum, we used the molar absorption coefficient reported for the monomeric radical. The linear combination corresponding to 25% of radical cation (precision ±5%), as shown in Figure 5a, provides a good agreement, not only for the spectral shape but also for the spectral intensity (right axis in $\Delta A/[e^-]_0$).

Dynamical Features. Typical examples of radical kinetics, determined at 500 and 600 nm, are shown in Figure 6. On the μs timescale, we observe that the differential absorbance at 500 nm decreases while that at 600 nm rises. The signals can be described by single exponential functions, $B_1 \exp(-t/\tau_2) + B_0$ and $B_1[1 - \exp(-t/\tau_2)] + B_0$, for the decrease and the rise, respectively, with the same time constant of 5 ± 1 μs. In view of our spectral analysis (Figure 5a), we assign the decay to the deprotonation of the radical cation and rise to the formation of the $(G\text{-}H2)^\bullet$ radical. The decays recorded on the ms timescale can be described by two-exponential functions $C_1 \exp(-t/\tau_3) + C_2 \exp(-t/\tau_4) + C_0$ with time constants of 2.6 ± 0.2 and 21 ± 2 ms. The latter are dominated by the disappearance of $(G\text{-}H2)^\bullet$ and $(G\text{-}H1)^\bullet$ radicals, respectively, as suggested by the time-resolved spectra in Figure 6b,c.

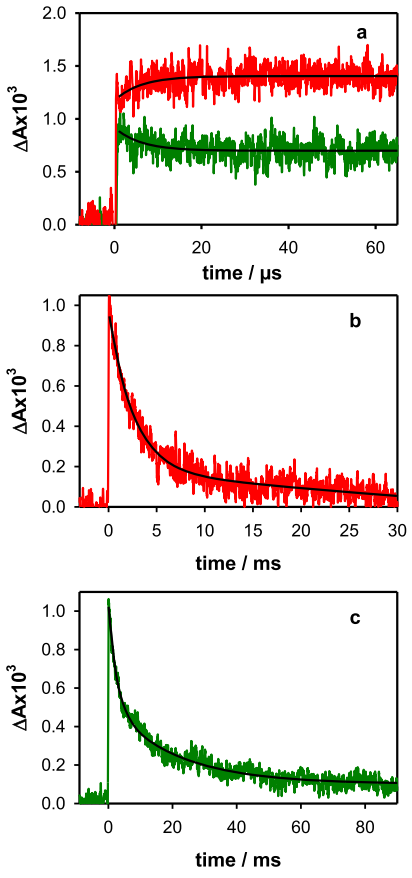

Figure 6. Normalized transient absorption signals recorded for $(TG4T)_4/Na^+$ at 500 nm (green) and 600 nm (red) at various timescales. Black lines correspond to fits with monoexponential (a; time constant 6 μs) and biexponential (b,c; time constants 2.6 and 21 ms) functions.

The time constants derived from the fits in Figure 6 do not necessarily correspond to "absolute lifetimes" of the various radicals. As largely documented in the literature, reaction kinetics in anisotropic structures follow nonexponential patterns that may extend over several decades of time (see, e.g., refs 50,51). In G-quadruplexes, guanine radicals have different local environments, depending, for instance, on their location in inner or outer tetrads. The picture is further complicated by dynamical disorder, related to continuous conformational changes,[52] as well as to motions of the Na^+ cations in the central cavity, occurring on the millisecond timescale.[53] It is worth noticing that the fluorescence decays of G-quadruplexes, probed over several orders of magnitude of time, also exhibit clearly multiscale decays (Figure 5 in ref 54).

The nonexponential kinetics of the $(TG4T)_4/Na^+$ radicals can be easily illustrated by the behavior of $(G)^{+\bullet}$. If the entire population of radical cations was decaying with the time constant of 5 ± 1 μs (Figure 6a), 67% should survive at 2.5 μs; but the spectra in Figure 5a indicate the presence of only 25%. This means that the major part of the radical cation population undergoes rapid deprotonation and our measurements on the μs timescale detect only the slower part of the process. This nonexponentiality is even more pronounced in the case of TEL21/Na^+, for which half of the radical cation population deprotonates on the millisecond timescale, while the other half deprotonates before 3 μs.[17]

Deprotonation of 25% of the radical cations in $(TG4T)_4/Na^+$ is completed within around 20 μs (Figure 6a). Based on the spectra in Figure 5b and using a molar absorption coefficient of 2100 mol^{-1} L cm^{-1} at 600 nm, determined for monomeric $(G\text{-}H2)^\bullet$ radicals,[46,48] we find that their concentration matches that of the ejected electrons. This means that the entire $(G)^{+\bullet}$ population undergoes deprotonation, with other types of reactions being negligible. This conclusion is confirmed by the lack of formation of 8-oxo-7,8-dihydro-2′-deoxyguanosine (8-oxodGuo) in $(TG4T)_4/Na^+$ samples irradiated at 266 nm by a continuous light source. As a matter of fact, 8-oxoGuo is a well-known reaction product issued from $(G)^{+\bullet}$,[55] whose quantitative determination may be achieved by mass spectrometry coupled to liquid chromatography. Such an analytical procedure, described in the Supporting Information, did not reveal any detectable formation of 8-oxodGuo. This shows that the corresponding quantum yield does not exceed 10^{-5}, which is 2 orders of magnitude lower that of the one-photon ionization yield (3.5×10^{-3}).

Using a value of 1500 mol^{-1} L cm^{-1} for the molar absorption coefficient of $(G\text{-}H1)^\bullet$ at 500 nm,[46] we find that when the $(G\text{-}H2)^\bullet \rightarrow (G\text{-}H1)^\bullet$ tautomerization is completed, within around 10 ms, only 40% of the initial radical population survives. Such a population is too low assuming that $(G\text{-}H2)^\bullet$ disappears according a monoexponential decay pattern and

DOI: 10.1021/acs.jpcb.9b02637
J. Phys. Chem. B 2019, 123, 4950−4957

$(G\text{-}H1)^{\bullet}$ is formed also following a monoexponential law. Besides the nonexponentiality of the process discussed above, another reason for the latter discrepancy could also be related to other reaction products formed directly from $(G\text{-}H2)^{\bullet}$ radicals. In our knowledge, the reactivity of $(G\text{-}H2)^{\bullet}$ radicals has not been explored so far.

The populations of the various $(TG4T)_4/Na^+$ and TEL21/Na^+ radicals present at selected times, expressed as molar fractions of the hydrated electron concentration, are shown in Table 1. Table 2 presents the time constants derived from the fits with exponential functions. Despite the lack of physical meaning of such fits, as they were performed over the same time domain, they allow comparison between the behavior of the two G-quadruplex scaffolds, when discussed in association with the populations in Table 1.

Table 1. Types of UV-Induced Guanine Radicals in $(TG4T)_4/Na^+$ at Selected Times; Their Populations Are Given as Fractions of the Initial Concentration of Detected Hydrated Electrons[a]

time	$(G)^{+\bullet}$	$(G\text{-}H2)^{\bullet}$	$(G\text{-}H1)^{\bullet}$
2 μs	0.25 [0.50]	0.75 [0.50]	
50 μs	0.00 [0.35]	1.02 [0.50]	
10 ms	0.00	0.00	0.40
180 ms	0.00	0.00	0.05 [0.06]

[a]Estimated error: ± 0.05. In brackets: values corresponding to TEL21/Na^+.[17]

Table 2. Lifetimes of Guanine Radicals Determined Experimentally for Two Different G-Quadruplex Scaffolds[a]

Process	$(TG4T)_4/Na^+$	TEL21/Na^+
slow part of deprotonation	5 ± 1 μs [−11/−16[c]]	1.2 ± 0.2 ms[b] [−22][c]
$(G\text{-}H2)^{\bullet}$ lifetime	2.6 ± 0.2 ms [−6]	1.2 ± 0.2 ms[d] [−4]
$(G\text{-}H1)^{\bullet}$ lifetime	21 ± 2 ms	50 ± 10 ms[d]

[a]In brackets: computed energy difference, in kcal mol^{-1}, corresponding to the deprotonation, E[$(G)^{+\bullet}$]-E[$(G\text{-}H2)^{\bullet}$], and tautomerization, E[$(G\text{-}H2)\bullet$]-E[$(G\text{-}H1)^{\bullet}$], processes. An energy of −262 kcal mol^{-1} is taken for the H^+ in aqueous solution.[56] [b]From ref 17. [c]localized/delocalized radical cations. [d]different values from those in ref 17 due to the different number of tetrads considered in the present QM model (3 instead of 2).

The most striking difference in the behavior of the two types of G-quadruplexes resides in the deprotonation dynamics of their cations. In view of both the population fractions surviving at 2 μs for $(TG4T)_4/Na^+$ and TEL21/Na^+ (0.25 vs 0.50) and the time constants determined for the slowest part of the deprotonation (5 μs vs 1.2 ms), it is clear that the deprotonation process is much more rapid for the tetramolecular structure. The considerably shorter lifetime of $(TG4T)_4/Na^+$ radical cations could account for the absence of 8-oxodGuo formation. In contrast, 7% of the longer living TEL21/Na^+ radical cations are transformed to 8-oxodGuo.[17] These dynamical features may also be correlated with energetic factors. The energy difference corresponding to $(G)^{+\bullet} \rightarrow (G\text{-}H2)^{\bullet}$ process computed at the QM/MM level for TEL21/Na^+ is twice as high as that of $(TG4T)_4/Na^+$ (Table 2), in qualitative agreement with faster deprotonation observed for the latter system. It is also worth noticing that according to Table 2, delocalization of the electron hole should increase its lifetime.

Contrary to deprotonation, the $(G\text{-}H2)^{\bullet} \rightarrow (G\text{-}H1)^{\bullet}$ tautomerization is slower for $(TG4T)_4/Na^+$ compared to TEL21/Na^+ (Table 1). The dynamics of this process could be associated with the relative stability of the two types of deprotonated radicals within each system. In this case, the energy difference between $(G\text{-}H2)^{\bullet}$ and $(G\text{-}H1)^{\bullet}$ radicals computed for $(TG4T)_4/Na^+$ is twice as high as that found for TEL21/Na^+ (Table 2). Finally, the lifetime of the $(G\text{-}H1)^{\bullet}$ found for $(TG4T)_4/Na^+$ is shorter than that determined for TEL21/Na^+ (Table 2). We explain this difference by the stability of the "normal", non-photoionized, G-quadruplex scaffolds, that is reflected in their melting curves. Under the same buffer conditions, the melting temperature of TEL21/Na^+ is 77 °C[17] while it is only 60 °C for $(TG4T)_4/Na^+$ (Figure S1).

CONCLUSIONS

The first important conclusion of the present study is that, like other DNA oligomers with a pronounced secondary structure, $(TG4T)_4/Na^+$ undergoes one-photon ionization at an energy lower by 2.7 eV than the ionization potential of nucleobases. The associated quantum yield (3.5×10^{-3}) is about three times higher than those reported previously for duplexes (18−20, 41) but 20% lower than that of TEL21/Na^+.[17] At the present state of knowledge, we cannot explain the different propensity of the various DNA strands in aqueous solution to undergo electron detachment upon irradiation with low-energy photons because the underlying mechanism is not known. Possible correlation with population of charge-transfer states involving different bases has been mentioned; such a scenario would imply charge separation, charge migration steps, and electron ejection from a radical anion.[20] A quite recent theoretical study reports that $\pi\sigma^*$ bonds may play a role in the photoionization process.[57] One could also imagine that the local structure and dynamics of water molecules are responsible for the decrease of the vertical ionization potential of a small fraction of nucleobases.[58] Collection of more experimental data, which is delicate and slow, combined to theoretical studies, is necessary to privilege one of these hypotheses.

Our second conclusion concerns the types of guanine radicals generated by photoionization; probed from 2 μs to 2 ms, they appear in the order $(G)^{+\bullet}$, $(G\text{-}H2)^{\bullet}$ and $(G\text{-}H1)^{\bullet}$. In connection with theoretical studies,[26,47] the spectrum of the radical cation indicates weak delocalization of the positive charge. In contrast, the spectrum of the deprotonated radical is practically identical to that of monomeric guanosine, both in intensity and in shape.[48] In fact, the experimental spectra of the radicals correspond to an average associated with highly anisotropic structures. Combination of quantum mechanical methods with molecular dynamics simulations should bring subtle information regarding the effect of local environment of radicals on their spectral properties.

The survival probabilities of the various $(TG4T)_4/Na^+$ radicals exhibit important differences compared to those determined previously for the TEL21/Na^+ radicals.[17] (i) Deprotonation of the radical cations is much faster, this behavior having been correlated to their lower reactivity toward 8-oxodGuo formation. (ii) The $(G\text{-}H2)^{\bullet} \rightarrow (G\text{-}H1)^{\bullet}$ tautomerization is slower, and (iii) the lifetime of $(G\text{-}H1)^{\bullet}$ is shorter. Such a comparison between tetramolecular and monomolecular G-quadruplexes that are formed in the presence of Na^+ ions brought light to the effect of topology

DOI: 10.1021/acs.jpcb.9b02637
J. Phys. Chem. B 2019, 123, 4950−4957

on the radical properties. It would be important to examine if these trends persist for other couples of parallel/antiparallel structures and, furthermore, examine the effect of the metal ions located in the central cavity of the G-quadruplex scaffolds.

We note that we found no report in the literature on direct UV-induced reactions of tetramolecular G-quadruplexes. Thus, the reaction products resulting from the two types of deprotonated radicals in $(TG4T)_4/Na^+$ remain to be determined.

■ ASSOCIATED CONTENT

Supporting Information

The Supporting Information is available free of charge on the ACS Publications website at DOI: 10.1021/acs.jpcb.9b02637.

(1) Melting curve, (2) computational model, (3) steady-state absorption spectra, (4) absorption spectra of $(G)^{+\bullet}$ in G-quadruplexes, and (5) continuous light irradiations and photoproduct analysis (PDF)

■ AUTHOR INFORMATION

Corresponding Author

*E-mail: dimitra.markovitsi@cea.fr. Phone: +33169084644.

ORCID

Roberto Improta: 0000-0003-1004-195X

Dimitra Markovitsi: 0000-0002-2726-305X

Author Contributions

The manuscript was written through contributions of all authors. All authors have given approval to the final version of the manuscript.

Notes

The authors declare no competing financial interest.

■ ACKNOWLEDGMENTS

This work was supported by the French National Research Agency [no ANR-12-BS08-0001-01, OPHID project]; Investissements d'Avenir LabEx PALM [ANR-10-LABX-0039-PALM]; Université Paris Saclay—programme D'Alembert 2016, no 10751 and the European Programme H2020 MSCA ITN [grant no. 765266—LightDyNAmics project] and used HPC resources from GENCI-IDRIS [grant 2017-A0030810262].

■ REFERENCES

(1) Plavec, J.; Sket, P., Diversity of DNA and RNA G-quadruplex structures. In *Biological Relevance & Therapeutic Applications of DNA- & RNA-Quadruplexes*, Monchaud, D., Ed.; Future Medicine Ltd: London, 2015; pp 22−36.

(2) Lipps, H. J.; Rhodes, D. G-quadruplex structures: in vivo evidence and function. *Trends Cell Biol.* **2009**, *19*, 414−422.

(3) Biffi, G.; Tannahill, D.; McCafferty, J.; Balasubramanian, S. Quantitative visualization of DNA G-quadruplex structures in human cells. *Nat. Chem.* **2013**, *5*, 182−186.

(4) Rhodes, D.; Lipps, H. J. G-quadruplexes and their regulatory roles in biology. *Nucleic Acids Res.* **2015**, *43*, 8627−8637.

(5) Livshits, G. I.; Stern, A.; Rotem, D.; Borovok, N.; Eidelshtein, G.; Migliore, A.; Penzo, E.; Wind, S. J.; Di Felice, R.; Skourtis, S. S.; Cuevas, J. C.; Gurevich, L.; Kotlyar, A. B.; Porath, D. Long-range charge transport in single G-quadruplex DNA molecules. *Nat. Nanotechnol.* **2014**, *9*, 1040−1046.

(6) Sha, R.; Xiang, L.; Liu, C.; Balaeff, A.; Zhang, Y.; Zhang, P.; Li, Y.; Beratan, D. N.; Tao, N.; Seeman, N. C. Charge splitters and charge transport junctions based on guanine quadruplexes. *Nat. Nanotechnol.* **2018**, *13*, 316−321.

(7) Fleming, A. M.; Ding, Y.; Burrows, C. J. Oxidative DNA damage is epigenetic by regulating gene transcription via base excision repair. *Proc. Natl. Acad. Sci. U.S.A.* **2017**, *114*, 2604−2609.

(8) Fouquerel, E.; Lormand, J.; Bose, A.; Lee, H.-T.; Kim, G. S.; Li, J.; Sobol, R. W.; Freudenthal, B. D.; Myong, S.; Opresko, P. L. Oxidative guanine base damage regulates human telomerase activity. *Nat. Struct. Mol. Biol.* **2016**, *23*, 1092−1100.

(9) Thazhathveetil, A. K.; Harris, M. A.; Young, R. M.; Wasielewski, M. R.; Lewis, F. D. Efficient Charge Transport via DNA G-Quadruplexes. *J. Am. Chem. Soc.* **2017**, *139*, 1730−1733.

(10) Choi, J.; Park, J.; Tanaka, A.; Park, M. J.; Jang, Y. J.; Fujitsuka, M.; Kim, S. K.; Majima, T. Hole Trapping of G-Quartets in a G-Quadruplex. *Angew. Chem., Int. Ed.* **2013**, *52*, 1134−1138.

(11) Candeias, L. P.; Steenken, S. Ionization of purine nucleosides and nucleotides and their components by 193-nm laser photolysis in aqueous solution: model studies for oxidative damage of DNA. *J. Am. Chem. Soc.* **1992**, *114*, 699−704.

(12) Kobayashi, K.; Tagawa, S. Direct observation of guanine radical cation deprotonation in duplex DNA using pulse radiolysis. *J. Am. Chem. Soc.* **2003**, *125*, 10213−10218.

(13) Adhikary, A.; Kumar, A.; Becker, D.; Sevilla, M. D. The guanine cation radical: investigation of deprotonation states by ESR and DFT. *J. Phys. Chem. B* **2006**, *110*, 24171−24180.

(14) Cadet, J.; Douki, T.; Ravanat, J.-L. Oxidatively generated damage to the guanine moiety of DNA: Mechanistic aspects and formation in cells. *Acc. Chem. Res.* **2008**, *41*, 1075−1083.

(15) Cadet, J.; Douki, T.; Ravanat, J.-L. Oxidatively Generated Damage to Cellular DNA by UVB and UVA Radiation. *Photochem. Photobiol.* **2015**, *91*, 140−155.

(16) Wu, L.; Liu, K.; Jie, J.; Song, D.; Su, H. Direct Observation of Guanine Radical Cation Deprotonation in G-Quadruplex DNA. *J. Am. Chem. Soc.* **2015**, *137*, 259−266.

(17) Banyasz, A.; Martínez-Fernández, L.; Balty, C.; Perron, M.; Douki, T.; Improta, R.; Markovitsi, D. Absorption of Low-Energy UV Radiation by Human Telomere G-Quadruplexes Generates Long-Lived Guanine Radical Cations. *J. Am. Chem. Soc.* **2017**, *139*, 10561−10568.

(18) Schroeder, C. A.; Pluhařová, E.; Seidel, R.; Schroeder, W. P.; Faubel, M.; Slavíček, P.; Winter, B.; Jungwirth, P.; Bradforth, S. E. Oxidation Half-Reaction of Aqueous Nucleosides and Nucleotides via Photoelectron Spectroscopy Augmented by ab Initio Calculations. *J. Am. Chem. Soc.* **2015**, *137*, 201−209.

(19) Banyasz, A.; Martínez-Fernández, L.; Improta, R.; Ketola, T.-M.; Balty, C.; Markovitsi, D. Radicals generated in alternating guanine-cytosine duplexes by direct absorption of low-energy UV radiation. *Phys. Chem. Chem. Phys.* **2018**, *20*, 21381−21389.

(20) Banyasz, A.; Ketola, T.; Martínez-Fernández, L.; Improta, R.; Markovitsi, D. Adenine radicals generated in alternating AT duplexes by direct absorption of low-energy UV radiation. *Faraday Discuss.* **2018**, *207*, 181−197.

(21) Banyasz, A.; Ketola, T.-M.; Muñoz-Losa, A.; Rishi, S.; Adhikary, A.; Sevilla, M. D.; Martinez-Fernandez, L.; Improta, R.; Markovitsi, D. UV-induced Adenine Radicals Induced in DNA A-tracts: Spectral and Dynamical Characterization. *J. Phys. Chem. Lett.* **2016**, *7*, 3949−3953.

(22) Burge, S.; Parkinson, G. N.; Hazel, P.; Todd, A. K.; Neidle, S. Quadruplex DNA: sequence, topology and structure. *Nucleic Acids Res.* **2006**, *34*, 5402−5415.

(23) Burge, S.; Parkinson, G. N.; Hazel, P.; Todd, A. K.; Neidle, S. Quadruplex DNA: sequence, topology and structure. *Nucleic Acids Res.* **2006**, *34*, 5402−5415.

(24) Visscher, K. J.; De Haas, M. P.; Loman, H.; Vojnovic, B.; Warman, J. M. Fast Protonation of Adenosine and of Its Radical Anion Formed by Hydrated Electron Attack; A Nanosecond Optical and Dc-conductivity Pulse Radiolysis Study. *Int. J. Radiat. Biol. Relat. Stud. Phys., Chem. Med.* **1987**, *52*, 745−753.

(25) Ma, J.; Wang, F.; Denisov, S. A.; Adhikary, A.; Mostafavi, M. Reactivity of prehydrated electrons toward nucleobases and nucleotides in aqueous solution. *Sci. Adv.* **2017**, *3*, No. e1701669.

(26) Martínez-Fernández, L.; Banyasz, A.; Markovitsi, D.; Improta, R. Topology controls the electronic absorption delocalization of electron hole in guanine quadruplexes. *Chem.—Eur. J.* **2018**, *24*, 15185−15189.
(27) Mergny, J.-L.; Phan, A.-T.; Lacroix, L. Following G-quartet formation by UV-spectroscopy. *FEBS Lett.* **1998**, *435*, 74−78.
(28) Amand, B.; Bensasson, R. Determination of triplet quantum yields by laser flash absorption spectroscopy. *Chem. Phys. Lett.* **1975**, *34*, 44−48.
(29) Zhao, Y.; Schultz, N. E.; Truhlar, D. G. Design of density functionals by combining the method of constraint satisfaction with parametrization for thermochemistry, thermochemical kinetics, and noncovalent interactions. *J. Chem. Theory Comput.* **2006**, *2*, 364−382.
(30) Zhao, Y.; Truhlar, D. G. Density functionals with broad applicability in chemistry. *Acc. Chem. Res.* **2008**, *41*, 157−167.
(31) Improta, R.; Barone, V. Excited states behavior of nucleobases in solution: insights from computational studies. *Top. Curr. Chem.* **2015**, *355*, 329−357.
(32) Improta, R.; Santoro, F.; Blancafort, L. Quantum Mechanical Studies on the Photophysics and the Photochemistry of Nucleic Acids and Nucleobases. *Chem. Rev.* **2016**, *116*, 3540−3593.
(33) Cornell, W. D.; Cieplak, P.; Bayly, C. I.; Gould, I. R.; Merz, K. M.; Ferguson, D. M.; Spellmeyer, D. C.; Fox, T.; Caldwell, J. W.; Kollman, P. A. A 2nd generation force-field for the simulation of proteins, nucleic acids, and organic molecules. *J. Am. Chem. Soc.* **1995**, *117*, 5179−5197.
(34) Dapprich, S.; Komáromi, I.; Byun, K. S.; Morokuma, K.; Frisch, M. J. A new ONIOM implementation in Gaussian98. Part I. The calculation of energies, gradients, vibrational frequencies and electric field derivatives. *J. Mol. Struct.: THEOCHEM* **1999**, *461−462*, 1−21.
(35) Miertuš, S.; Scrocco, E.; Tomasi, J. Electrostatic interaction of a solute with a continuum - A direct utilization of abinitio molecular potentials for the prevision of solvent effects. *Chem. Phys.* **1981**, *55*, 117−129.
(36) Tomasi, J.; Mennucci, B.; Cammi, R. Quantum mechanical continuum solvation models. *Chem. Rev.* **2005**, *105*, 2999−3094.
(37) Laughlan, G.; Murchie, A.; Norman, D.; Moore, M.; Moody, P.; Lilley, D.; Luisi, B. The high-resolution crystal-structure of parallel-stranded guanine tetraplex. *Science* **1994**, *265*, 520−524.
(38) Kumar, A.; Sevilla, M. D. Excited States of One-Electron Oxidized Guanine-Cytosine Base Pair Radicals: A Time Dependent Density Functional Theory Study. *J. Phys. Chem. A* **2019**, *123*, 3098−3108.
(39) Torche, F.; Marignier, J.-L. Direct Evaluation of the Molar Absorption Coefficient of Hydrated Electron by the Isosbestic Point Method. *J. Phys. Chem. B* **2016**, *120*, 7201−7206.
(40) Gauduel, Y.; Migus, A.; Chambaret, J. P.; Antonetti, A. Femtosecond Reactivity of Electron in Aqueous Solutions. *Rev. Phys. Appl.* **1987**, *22*, 1755−1759.
(41) Buxton, G. V.; Greenstock, C. L.; Helman, W. P.; Ross, A. B. Critical review of rate constants for reactions of hydrated electrons, hydrogen atoms and hydroxyl radicals (.OH/O.-) in aqueous solution. *J. Phys. Chem. Ref. Data* **1988**, *17*, 513−886.
(42) Nikogosyan, D. N.; Oraevsky, A. A.; Letokhov, V. S.; Arbieva, Z. K.; Dobrov, E. N. Two-step picosecond UV excitation of polynucleotides and energy transfer. *Chem. Phys.* **1985**, *97*, 31−41.
(43) Görner, H. New trends in photobiology. *J. Photochem. Photobiol., B* **1994**, *26*, 117−139.
(44) Crespo-Hernández, C. E.; Arce, R. Near threshhold photo-oxidation of dinucleotides containing purines upon 266 nm nanosecond laser excitation. The role of base stacking, conformation and sequence. *J. Phys. Chem. B* **2003**, *107*, 1062−1070.
(45) Marguet, S.; Markovitsi, D.; Talbot, F. One and two photon ionization of DNA single and double helices studied by laser flash photolysis at 266 nm. *J. Phys. Chem. B* **2006**, *110*, 11037−11039.
(46) Candeias, L. P.; Steenken, S. Stucture and acid-base properties of one-electron-oxidized deoxyguanosine, guanosine, and 1-methyl-guanosine. *J. Am. Chem. Soc.* **1989**, *111*, 1094−1099.
(47) Sun, W. M.; Varsano, D.; Di Felice, R. Effects of G-Quadruplex Topology on Electronic Transfer Integrals. *Nanomaterials* **2016**, *6*, 184.
(48) Chatgilialoglu, C.; Caminal, C.; Altieri, A.; Vougioukalakis, G. C.; Mulazzani, Q. G.; Gimisis, T.; Guerra, M. Tautomerism in the guanyl radical. *J. Am. Chem. Soc.* **2006**, *128*, 13796−13805.
(49) Rokhlenko, Y.; Cadet, J.; Geacintov, N. E.; Shafirovich, V. Mechanistic Aspects of Hydration of Guanine Radical Cations in DNA. *J. Am. Chem. Soc.* **2014**, *136*, 5956−5962.
(50) Blumen, A.; Klafter, J.; Zumofen, G., Models for reaction dynamics in glasses. In *Optical Spectroscopy of Glasses*; Zschokke, I., Ed.; Reidel Publishing Co., 1986; pp 199−265.
(51) Cichos, F.; Vonborczyskowski, C.; Orrit, M. Power-law intermittency of single emitters. *Curr. Opin. Colloid Interface Sci.* **2007**, *12*, 272−284.
(52) Cragnolini, T.; Chakraborty, D.; Sponer, J.; Derreumaux, P.; Pasquali, S.; Wales, D. J. Multifunctional energy landscape for a DNA G-quadruplex: An evolved molecular switch. *J. Chem. Phys.* **2017**, *147*, 152715.
(53) Šket, P.; Plavec, J. Tetramolecular DNA Quadruplexes in Solution: Insights into Structural Diversity and Cation Movement. *J. Am. Chem. Soc.* **2010**, *132*, 12724−12732.
(54) Changenet-Barret, P.; Hua, Y.; Gustavsson, T.; Markovitsi, D. Electronic excitations in G-quadruplexes formed by the human telomeric sequence: a time-resolved fluorescence study. *Photochem. Photobiol.* **2015**, *91*, 759−765.
(55) Kasai, H.; Yamaizumi, Z.; Berger, M.; Cadet, J. Photosynsitized formation of 7,8-dihydro-8-oxo-2'-deoxoguanosine (8-hydroxy-2'-deoxoguanosine) in DNA by riboflavin - a non singlet oxygen mediated reaction. *J. Am. Chem. Soc.* **1992**, *114*, 9692−9694.
(56) Tawa, G. J.; Topol, I. A.; Burt, S. K.; Caldwell, R. A.; Rashin, A. A. Calculation of the aqueous solvation free energy of the proton. *J. Chem. Phys.* **1998**, *109*, 4852−4863.
(57) Karsili, T. N. V.; Marchetti, B.; Ashfold, M. N. R. The role of (1)pi sigma* states in the formation of adenine radical-cations in DNA duplexes. *Chem. Phys.* **2018**, *515*, 464−471.
(58) Laage, D.; Elsaesser, T.; Hynes, J. T. Water Dynamics in the Hydration Shells of Biomolecules. *Chem. Rev.* **2017**, *117*, 10694−10725.

DOI: 10.1021/acs.jpcb.9b02637
J. Phys. Chem. B 2019, 123, 4950−4957